Ultrafast Vibrational Dynamics of a Solute Correlates with Dynamics of the Solvent

Vivian F. Crum, Laura M. Kiefer and Kevin J. Kubarych*
Department of Chemistry, University of Michigan, 930 N. University Ave., Ann Arbor, MI 48109
* Email: kubarych@umich.edu

ABSTRACT

Two-dimensional infrared (2D-IR) spectroscopy is used to measure the spectral dynamics of the metal carbonyl complex, cyclopentadienyl manganese tricarbonyl (CMT) in a series of linear alkyl nitriles. 2D-IR spectroscopy provides direct readout of solvation dynamics through spectral diffusion, probing the decay of frequency correlation induced by fluctuations of the solvent environment. 2D-IR simultaneously monitors intramolecular vibrational energy redistribution (IVR) among excited vibrations, which can also be influenced by the solvent through the spectral density rather than the dynamical friction underlying solvation. Here, we report that the CMT vibrational probe reveals solvent dependences in both the spectral diffusion and the IVR time scales, where each slows with increased alkyl chain length. In order to assess the degree to which solute-solvent interactions can be correlated with bulk solvent properties, we compared our results with low-frequency dynamics obtained from optical Kerr effect (OKE) spectroscopy—performed by others—on the same nitrile solvent series. We find excellent correlation between our spectral diffusion results and the orientational dynamics time scales from OKE. We also find a correlation between our IVR time scales and the amplitudes of the low-frequency spectral densities evaluated at the 90-cm⁻¹ energy difference, corresponding to the gap between the two strong vibrational modes of the carbonyl probe. 2D-IR and OKE provide complementary perspectives on condensed phase dynamics, and these findings provide experimental evidence that, at least at the level of dynamical correlations, some aspects of a solute vibrational dynamics can be inferred from properties of the solvent.

INTRODUCTION

Although there has been extensive research on solvation dynamics and solute-solvent interactions, the influence of solvents on chemical reactions are still relatively complicated and unpredictable. There is a long tradition in chemical physics of employing solutes to serve as spectroscopic probes, such as fluorescent dyes, taking advantage of convenient spectral properties to extract solvation dynamics, for example, by monitoring the time-resolved Stokes shift. With the advent of two-dimensional infrared (2D-IR) spectroscopy, comparably smaller solutes have proven useful for accessing solvation dynamics without introducing complexities associated with electronic excitation. Whereas visible transitions are delocalized over much of the probe molecule, vibrational probes can be localized over a few atoms, providing some enhancement in spatial resolution, albeit with a loss of temporal dynamic range. Regardless of the nature of the solute or the spectroscopic probe, there always remains an unknown perturbation due to potentially specific solute-solvent interactions complicating general conclusions using any kind of probe. A question that remains open is whether it is possible to predict solute dynamics, or the dynamics sensed by the solute, based only, or primarily, on the properties of the solvent.

In our first effort to study solvation dynamics using vibrational probes, we studied a transition metal complex, dimanganese decacarbonyl [Mn₂(CO)₁₀ (DMDC)], in a series of linear alcohols.¹ Taking advantage of the ability to measure the frequency fluctuation correlation function [FFCF, $C(t) = \langle \delta \omega(0) \delta \omega(t) \rangle$] by analyzing the 2D-IR spectra, we found a linear dependence of the spectral diffusion time scale on solvent chain length. Because the viscosity of the solvents also depends on chain length, we

naturally also found a linear dependence of the solvation dynamics time scale on the solvent viscosity. Using another metal carbonyl complex, cyclopentadienyl manganese tricarbonyl (CMT), in the same alcohol series, we found the same linear chain length/viscosity dependence, even when the probe molecule was contained within a cyclodextrin inclusion complex.²

These examples might suggest a straightforward link between spectral diffusion and bulk solvent properties, such as viscosity. There are, however, many counterexamples where we, and others, find a distinct lack of simple correlation with solvent viscosity. Massari et al. studied Vaska's complex and its adducts in a series of chemically unrelated solvents [i.e. benzene, chloroform, and dimethyl formamide (DMF)], finding a dependence on the solvent's acceptor number, which is a measure of Lewis acidity.^{3,4} We studied a probe complex, Re₂(CO)₁₀, in 1,2-hexanediol which is a glass forming liquid with a glass transition near room temperature.⁵ We found stretched-exponential spectral diffusion above and near the glass transition, with a pronounced slowdown close to the transition temperature, but over a very large viscosity range in approach to the glass transition, the spectral diffusion is actually independent of temperature (and viscosity). In an entirely separate context, we measured spectral diffusion dynamics of a ruthenium dicarbonyl probe conjugated to the protein hen egg white lysozyme in D₂O/glycerol mixtures, finding a monotonic, if not simply linear, dependence on glycerol concentration and only observed minor increases in spectral diffusion times (~3-fold) despite drastic differences in solvent mixture viscosity (~100fold increase). In solvent mixtures, Kwak et al. found composition dependent spectral diffusion dynamics reflecting exchange of dissimilar solvent shell species.⁷ A similar result was found for water/DMSO mixtures, where solvent exchange introduces a slower phase in spectral diffusion and in orientational relaxation. Using BCT labeled biotin, we studied the spectral diffusion dynamics in water/DMF mixtures, finding a DMF mole fraction dependence that we could explain using a model of solvent exchange and preferential solvation. ⁹ There are many dynamic fluorescence experiments that report slower solvation in solvent mixtures than in either pure solvent. 10-13 In another mixed-solvent study, we examined the spectral diffusion dynamics of the CO₂ reduction catalyst Re(bpy)(CO)₃Cl (bpy = bipyridyl) in tetrahydrofuran(THF)/triethanolamine(TEOA) solutions, finding a complex composition dependence where the slowest spectral diffusion occurs at a 20% (v/v) solution of TEOA in THF.¹⁴ Similar to the biotin example, we were able to explain this nonmonotonic solvation dynamics trend as resulting from solvent exchange. In various solvents used in electro- and photocatalysis, Re(bpy)(CO)₃Cl exhibits spectral diffusion that depends on the donor number or nucleophilicity of the solvent, but, although not initially identified, also correlates with viscosity.¹⁵ Viscosity is a bulk property of the solvent that may not be expected to reflect the true microscopic molecular dynamics on the length scale of individual molecules, but there are nevertheless cases where spectral diffusion correlates with the viscosity.

Two themes emerge from previous solvation dynamics studies using 2D-IR. Firstly, there are classes of dynamic motion that do not admit a hydrodynamic description, being subject instead to the faster fluctuations of local structure such as cages and other specific solvent configurations. The temperature-independent spectral diffusion in the glass forming liquid is an example of this dynamic decoupling.⁵ Secondly, there is the very important, but easily overlooked, chemical aspect of the solvents. That is, they are not continuum dielectrics and have specific interactions, both with the solute and among the solvent molecules themselves. It appears to be the case that the chemical nature of the solvent can be more important for determining the spectral diffusion dynamics than is hydrodynamic transport (i.e. viscosity). One corollary is that within a series of chemically homologous solvents, the viscosity may be a good predictor of spectral diffusion. It is this latter point that we seek to address in the present study of solvation dynamics in the nitrile series.

Alkyl Nitrile Solvents. Unlike alcohols, alkyl nitriles are aprotic and therefore cannot hydrogen bond in the neat liquid. The nitrogen of the nitrile group is capable of acting as a hydrogen bond acceptor with hydrogen bond donors, making them soluble in protic solvents. As an example of the compatibility with protic solvents, Hochstrasser *et al.* found evidence of chemical exchange between free ACN and a

hydrogen bonded ACN/methanol complex using two-dimensional infrared (2D-IR) spectroscopy.¹⁸ As a series, the alkyl nitriles have been studied in various contexts. Although ACN is a common solvent implemented in organic chemistry and electrochemistry, several nitriles including propionitrile (PCN) have been investigated in understanding solvent influences on the reduction of metal ions.¹⁹ Longer chained nitriles, such as valeronitrile (VCN), are attractive solvents for dissolving the electrolyte lithium bis(fluorosulfonyl)imide for use in lithium batteries since they are less hygroscopic than the shorter chained nitriles.²⁰ As a series, solvent effects of the alkyl nitriles have been investigated in a variety of contexts ranging from fluorescence emission of cationic-exciplexes²¹, barrier crossing reactions²², contact radical ion pair dynamics^{23,24}, isomerization rates²⁵, rotational diffusion dynamics²⁶, and formation of the triplet state of a metal porphine²⁷.

Intramolecular Vibrational Redistribution. In addition to spectral diffusion, 2D-IR spectroscopy directly measures time scales for intramolecular vibrational energy redistribution (IVR) by monitoring cross peak amplitudes as a function of the waiting time (t_2) between the excitation and detection pulses. Rapid energy exchange between vibrational modes due to IVR results in a growth in the cross peak amplitudes. Excess vibrational energy from this process is transferred to and from the bath. The principal theory used to describe IVR is essentially Fermi's golden rule, where energy in the donor state, an excited vibration, transfers to an acceptor vibration, with the energy balance provided by, or transferred to the bath.^{28,29} The "bath" may refer to the solvent or to intramolecular degrees of freedom that we do not probe directly with spectroscopy. The rate of IVR depends on the anharmonic coupling among the vibrations of the solute, and on the low-frequency liquid phonon modes (< 200 cm⁻¹) of the bath.^{28,30} We do not anticipate significant changes to the solute vibration's density of states as a function of solvent, so the density of states contribution that we anticipate being solvent dependent is the low-frequency spectral density of the solvent itself. The mode-to-mode coupling is the anharmonic coupling of the solute vibrations, and we similarly expect little solvent dependence of that, especially given the near complete solvent insensitivity of the linear and 2D-IR spectra that we report below. According to Fermi's golden rule, the rate of this transfer process is directly proportional to the spectral density of these liquid phonon modes at the energy difference between the coupled higher frequency vibrations.^{30,31} Though not widely analyzed in 2D-IR, we have found that solvent dependent IVR is not uncommon, and can reveal surprising aspects of solvation, such as solvent-specific hydrogen bonding and solvent packing.³² Here, we observe an alkyl chain length dependent IVR trend that we can relate to the solvent spectral densities obtained from optical Kerr effect (OKE) spectroscopy.

Orientational Dynamics and Reduced Spectral Densities from Optical Kerr Effect Spectroscopy. A technique that complements 2D-IR spectroscopy is optical Kerr effect, or OKE, spectroscopy, which probes the low-frequency anisotropic response via the time-dependent transient birefringence.³³ The collective orientational correlation function is fitted to a sum of exponential decays, where the extracted time constants describe aspects of the orientational diffusion. OKE has been widely applied to characterizing the orientational dynamics of neat liquids^{33–36} and even liquids on surfaces.³⁷ Because spectral diffusion arises from electrostatically-induced frequency fluctuations of the probe, we expect the orientational diffusion of the solvent molecules to be a major contributor to the spectral diffusion time scale. Pairing orientational diffusion of the solvent with spectral diffusion of the solute gives a complementary picture of solvation dynamics. Indeed, a seminal example of this approach was adopted nearly 30 years ago by Cho et al. comparing dynamic Stokes shift solvation of a dye in solution with OKE of the solvent alone.³⁸ In that case, the parameters extracted from a fit to the OKE response could be used as input to the corresponding non-equilibrium solvation response, producing essentially quantitative agreement. Though certainly a convincing example of the complementary perspectives provided by the two methods of studying solvation, electronic transitions are highly delocalized and would be the most likely candidates for correlating with collective low-frequency modes of a liquid. In the case of localized vibrations, it is not necessarily obvious that delocalized liquid dynamics would correlate spectral diffusion. Although these

techniques measure different processes, correlations made between the findings from OKE and findings from 2DIR spectroscopy signify that there is a connection between the two processes.

OKE spectroscopy can also be used to complement IVR information obtained from 2D-IR spectroscopy. Because OKE spectroscopy probes the low-frequency Raman response, it should be possible to characterize the density of liquid phonon modes that drive IVR in the solute. The so-called "reduced spectral density" (RSD) is the imaginary part of the Fourier transform of the time-domain signal from which the orientational component has been removed.^{39,40} These spectra are generally in the frequency range <500 cm⁻¹, covering the range of frequencies of the liquid phonon modes. Thus, in theory, the amplitudes of the RSD spectra are related to the spectral density of the liquid phonon modes, which is directly proportional to the rate of IVR according to Fermi's golden rule and are obtained via cross peak amplitudes in 2D-IR spectroscopy.

In this work, we report spectral diffusion and IVR of CMT in a series of alkyl nitriles via 2D-IR spectroscopy. As mentioned previously, metal carbonyls, including CMT, are excellent infrared probes in solvation studies due to their sensitivity to their environment. Unlike fluorescent dyes, many metal carbonyls are catalysts, such as $Re(bpy)(CO)_3Cl$, or resemble catalysts. ^{41,42} Metal tricarbonyls in particular, such as CMT, benzene chromium tricarbonyl, cyclopentadienyl rhenium tricarbonyl, and a large class of rhenium tricarbonyls, have been used as vibrational and x-ray spectroscopic labels. ^{2,9,43–46} Similar to DMDC and CMT in the alkyl alcohols^{1,2}, we observe viscosity-dependent spectral diffusion of CMT in alkyl nitriles. We also uncover correlations between our findings and OKE measurements on the alkyl nitriles.

MATERIALS AND EXPERIMENTAL METHODS

Sample Preparation. $(C_5H_5)Mn(CO)_3$ (CMT), acetonitrile [CH₃CN (ACN)], propionitrile [CH₃CH₂CN (PCN)], butyronitrile [CH₃(CH₂)₂CN (BCN)], valeronitrile [CH₃(CH₂)₃CN (VCN)], and hexanenitrile [CH₃(CH₂)₄CN (HCN)] were purchased from Sigma Aldrich and were used without any further purification. All samples were prepared to have a CMT concentration of ~10 mM and were sonicated before each experiment to reduce scattering.

2D-IR Spectroscopy. The experimental setup is discussed elsewhere. 47,48 Briefly, 100 fs pulses centered at 800 nm are generated by a Ti:sapphire regenerative amplifier and sent into two independent β-barium borate (BBO) optical parametric amplifiers (OPAs). The signal outputs from the OPAs drive two separate AgGaS difference frequency generation (DFG) crystals to generate mid-IR pulses (~2025 cm⁻¹; 125 cm⁻¹ full-width at half-maximum). There are four beams created for our experiments: two pump beams, a probe and a local oscillator (LO). The two pump beams and the probe are arranged in a noncollinear box geometry and interact with the sample. The resultant signal is mixed collinearly with a LO to allow for heterodyne detection. Sum frequency generation (SFG) between the signal and a chirped pulse centered at 800 nm in a 5% MgO-doped LiNbO₃ crystal upconverts the mid-IR signal into the visible, allowing for the use of a CCD camera as a detector synchronized with the 1 kHz repetition rate amplifier. In a typical 2D-IR experiment, the t_1 delay between the first two pump pulses is continuously scanned using ZnSe wedges at a range of fixed waiting times (t_2) between the second and third pulses. The detection frequencies (ω_3) are directly measured by the spectrometer while the excitation frequencies (ω_1) are obtained by Fourier transforming with respect to t_1 .

There are two phase-matched signals that are measured in our 2D-IR experiments: rephasing ($\mathbf{k}_r = -\mathbf{k}_1 + \mathbf{k}_2 + \mathbf{k}_3$) and non-rephasing ($\mathbf{k}_{nr} = \mathbf{k}_1 - \mathbf{k}_2 + \mathbf{k}_3$). The difference between the two arises from the coherences produced during the coherence evolution time (t_1) and the time after the third pulse interacts with the sample (t_3). In our setup, the two pathways are isolated by switching the ordering of the first two pulses. A key observable obtained via 2D-IR spectroscopy is the frequency fluctuation correlation function [(FFCF), $C(t) = \langle \delta\omega(0)\delta\omega(t)\rangle$]. Interactions between the solute and its environment lead to slight shifts in frequency over time. For ergodic systems, the vibrational probe will essentially lose memory of its initial frequency, leading to a decay of the FFCF. Our experiments do not measure the FFCF directly but rather, they measure the inhomogeneity index, $II(t_2)$:

$$II(t_2) = \frac{A_R(t_2) - A_{NR}(t_2)}{A_R(t_2) + A_{NR}(t_2)}$$

 $II(t_2) \,=\, \frac{A_R(t_2)\,-\,A_{NR}(t_2)}{A_R(t_2)\,+\,A_{NR}(t_2)}$ where A_R and A_{NR} are the absolute value of the rephasing and non-rephasing amplitudes respectively at each fixed t2 time delay. The inhomogeneity index is an amplitude-based method of determining the reversibility of the frequency distribution at a given t_2 waiting time. The transformation between the normalized FFCF and the $II(t_2)$ is given by the following equation⁴⁹:

$$C(t_2) = \sin\left[\frac{\pi II(t_2)}{2}\right]$$

We have recently reported an extensive comparison between the FFCF obtained using the inhomogeneity index and that obtained using the more widely used center line slope method. 49 Both approaches produce similar t₂-dependent decays.

RESULTS AND DISCUSSION

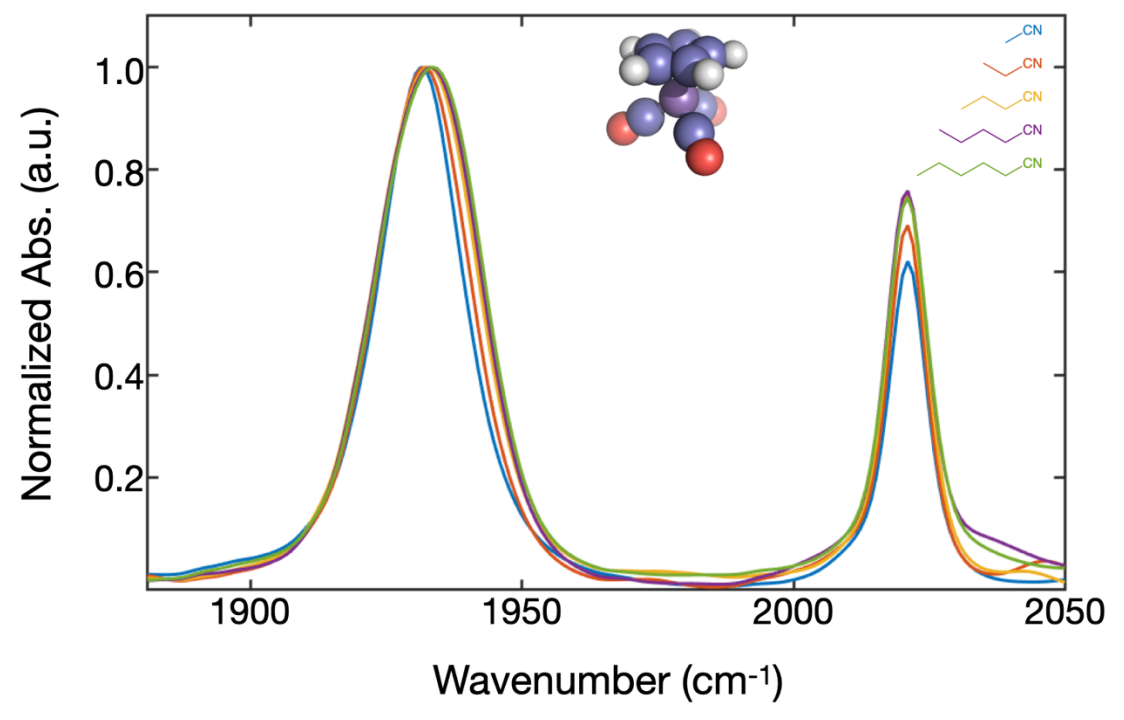


Figure 1. Normalized FTIR spectra of CMT in the series of alkyl nitriles. The structure of CMT is shown in between the two bands. The higher frequency band position does not depend on the solvent chain length, but the lower frequency band shows a slight enhancement in the red side, suggesting an asymmetric broadening likely arising from the lowered symmetry resulting in a slight breaking of the degeneracy of the two asymmetric modes. It is noteworthy that the spectra broaden with increased solvent alkyl chain length. The opposite trend is observed in alcohols.

FTIR spectra of CMT in various alkyl nitriles were measured and are shown in Fig. 1. CMT contains two vibrational bands in its FTIR spectrum: a doubly degenerate asymmetric band (~1930 cm⁻¹) and a higher frequency symmetric mode (~2021 cm⁻¹). Previously we have studied several metal carbonyl complexes in alcohol solvent series, finding that the carbonyl stretches exhibit blue-shifted and narrower linewidths with increased alcohol solvent chain length. 1,2 CMT follows this trend in alkyl alcohols, 2 but the band shifts are much less pronounced in the alkyl nitriles. Shifts in the vibrational bands of CMT in the alcohol series are mainly due to the hydrogen bonding between the solvent molecules and the carbonyls,⁵⁰ which is not present in the aprotic alkyl nitriles. Thus, the lack of significant shifts of CMT in

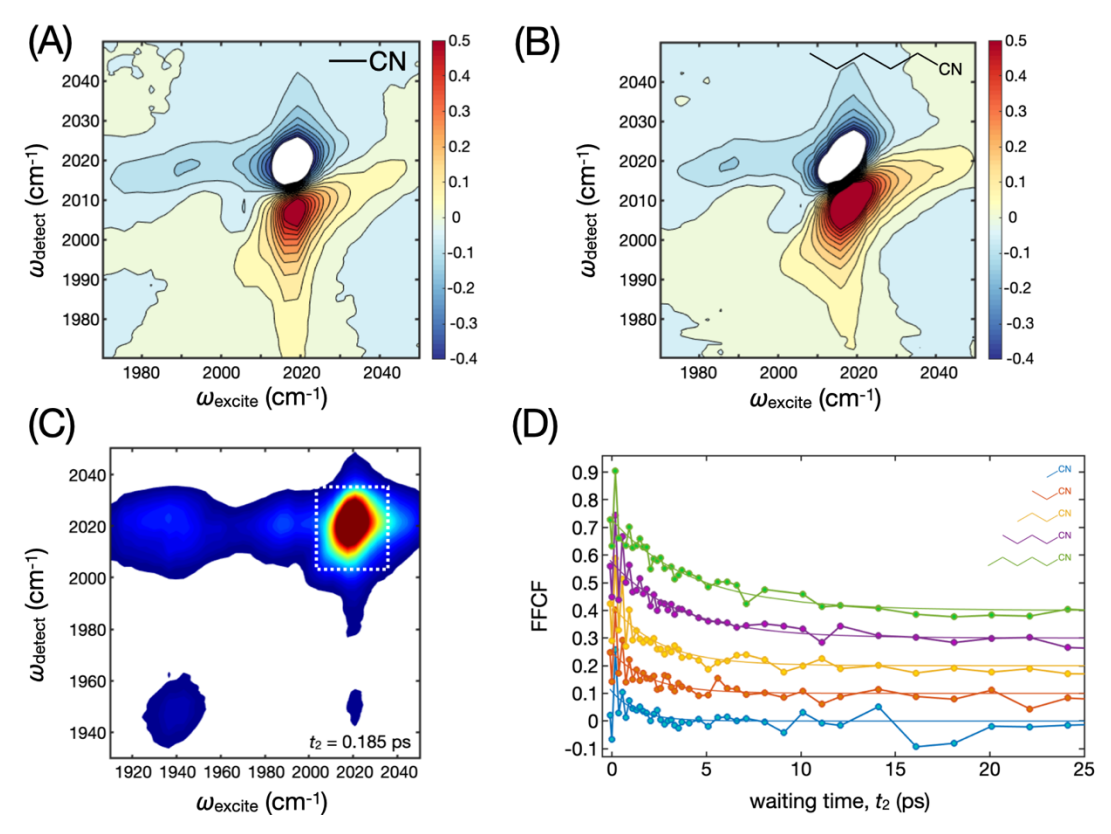


Figure 2. Absorptive spectra the symmetric mode of CMT in the shortest (A) and longest (B) chain nitriles at the same t_2 waiting time (t_2 = 0.185 ps) exhibit different lineshapes. (C) The 2D rephasing spectra of CMT in the longest chain nitrile at the waiting time (t_2) = 0.185 ps is shown. FFCFs are obtained by selecting the symmetric mode (white box) and calculating its volume. (D) All the FFCFs are fitted to single exponentials to extract spectral diffusion times (the offsets are added for clarity).

the various nitriles is perhaps unsurprising. The primary difference among the spectra of CMT in the nitriles is related to the linewidth of the asymmetric band, where we find the full-width at half-maximum (FWHM) increases with alkyl chain length. Since the asymmetric band is degenerate, the changes in the FWHM signify a slight disruption in the symmetry of the molecule and the two asymmetric modes losing their degeneracy. Why this symmetry lowering is more pronounced in the longer chain nitriles is not obvious. We have performed DFT calculations of the harmonic vibrational frequencies using polarizable continuum solvent models of all the nitrile solvents investigated experimentally, and we do not observe a symmetry lowering evidenced by a solvent-dependent splitting of the low-frequency band. The lack of continuum solvent dependence suggests the symmetry lowering is due to solvent packing or specific interactions with the solute.

An absorptive spectrum at a fixed waiting time is generated by adding the real components of the phased rephasing and non-rephasing spectra at that waiting time. Phasing rephasing and non-rephasing spectra is accomplished by multiplying each pathway by a correction factor that accounts for the inability to accurately define $t_1 = 0$ and $t_3 = 0$ and for phase differences between rephasing and non-rephasing.^{51,52} Absorptive spectra of the symmetric mode of CMT in the shortest (ACN) and the longest (HCN) chain nitrile are shown in **Fig. 2A and Fig. 2B** respectively. Qualitatively, the symmetric peak of CMT in HCN (**Fig. 2A**) is more elongated compared to CMT in ACN (**Fig. 2B**), already suggesting that the spectral diffusion is solvent dependent. Because we focus on the spectral dynamics of the higher frequency mode, our excitation and detection pulses are tuned to overlap that band, which causes the peaks involving the lower frequency band to be smaller in amplitude. The coupled carbonyl vibrations share a common ground

state, thus inherent cross peaks arise in the 2D spectra of CMT (**Fig. 2C**). Although both bands are excited and detected, the degeneracy of the asymmetric band may pose problems in obtaining and interpreting spectral diffusion due to the fact that the asymmetric modes can exchange energy and also may exhibit spectral diffusion of different time scales. Thus, only the FFCFs of the symmetric mode will be considered here. FFCFs are obtained for each solvent using Eq. 1. The rephasing and non-rephasing amplitudes are obtained by creating a box around the peak of interest and integrating the volume of that peak (**Fig. 2C**). Each calculated FFCF decay of the symmetric mode is fitted to a single exponential (without a constant offset) to extract spectral diffusion times (**Fig. 2D**). The FFCF decay times obtained from the fits are summarized in **Table 1**.

Table 1: Summary of the spectral diffusion times and time compression factors from fitting the FFCFs and the IVR time scales from fitting the cross peak to diagonal peak ratios for CMT in each solvent.

Solvent	ACN	PCN	BCN	VCN	HCN
FFCF decay time (ps)	1.3 ± 1.04	2.0 ± 0.97	2.5 ± 0.98	3.6 ± 1.10	4.2 ± 0.96
Time compression factor	1 ± 0.2	1.5 ± 0.3	2.3 ± 0.3	3.5 ± 0.4	6 ± 0.5
IVR times (ps)	5.9 ± 0.68	8.8 ± 1.3	11.79 ± 2.1	12.17 ± 2.5	13.53 ± 3.1

The values from the exponential fits give quantitative insight on the FFCF decays, but these values are not necessarily unique or free of uncertainty. Because our laser bandwidth is broad enough to excite and detect both vibrational bands, the non-rephasing diagonal signal amplitudes exhibit oscillations due to the coherent excitation of both states.^{1,53} The inhomogeneity index that we compute is constructed from the difference of the non-oscillatory rephasing and oscillator non-rephasing signals, leading to oscillations

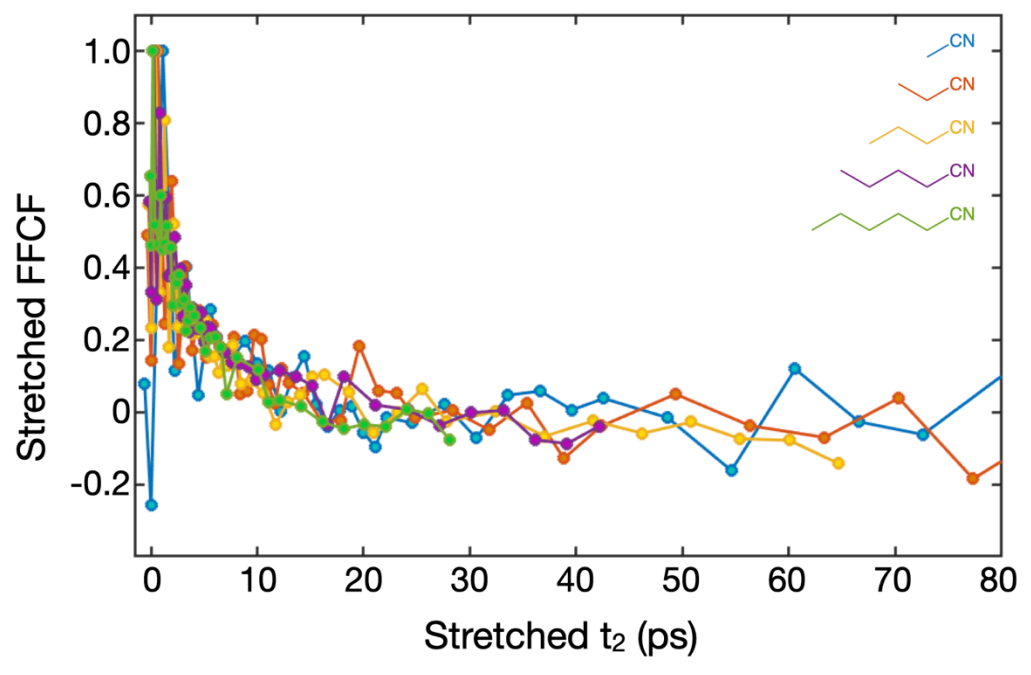


Figure 3. A master curve is created by rescaling the amplitudes and time scales of the FFCFs. The time compression factors obtained from this alternative fitting procedure describe relative spectral diffusion times.

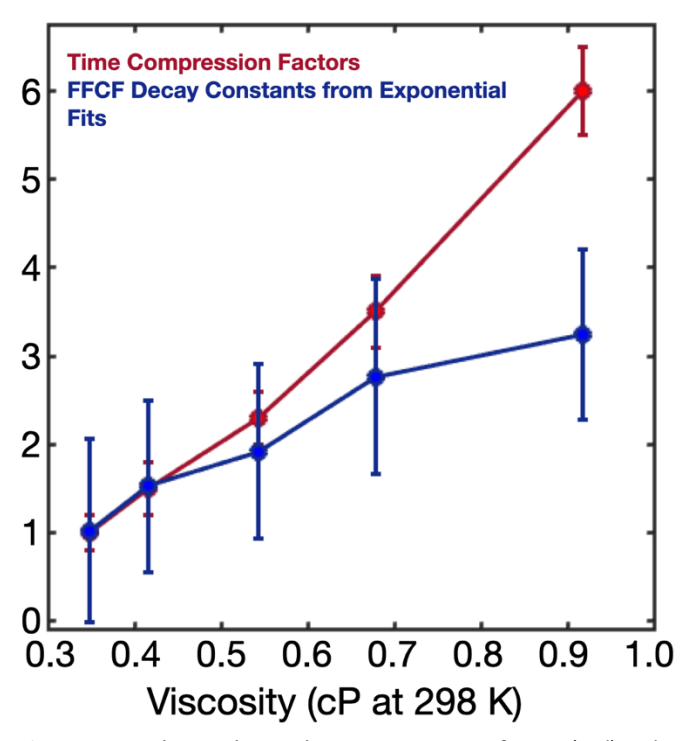


Figure 4. Correlation plots with time compression factors (red) and spectral diffusion times (blue) against solvent viscosities show linear correlations. Each plot is scaled to start at the same point to highlight the differences between the plots and their linearity.

in the extracted FFCFs. In the FFCFs, these oscillatory features are most prominent at waiting times less than ~10 ps (See Supplementary Materials, SM). I These earlytime oscillations tend to make the FFCFs appear to be noisy because we do not oversample the oscillations. The more significant challenge is that these oscillations introduce uncertainty in the exponential fits. Thus, we used another fitting procedure to eliminate any inherent bias introduced by imposing exponential decays.^{5,54,55} A master curve is generated by rescaling the amplitudes and the time axes of the FFCF decays and superimposing each rescaled decay onto a single curve, i.e. $C(t_2) \rightarrow \alpha C(\tau t_2)$ where τ is a time compression factor and α is an amplitude scaling factor (Fig. 3). The time compression factors are summarized in Table 1. The time compression factors compare spectral diffusion time scales rather than relying on exponential fits to obtain a definite spectral diffusion time. This alternative method produces a similar trend seen with the exponential fits.

Both procedures indicate that the spectral diffusion of CMT is solvent dependent. Previously we have found viscosity-dependent spectral diffusion times with metal carbonyls within the linear alkane series and within the linear alcohol solvent series, including CMT.^{1,2,56} Similarly to the alcohols, the viscosities of the alkyl nitriles increase with alkyl chain length.^{23,26,57} Plots comparing the viscosities of the alkyl nitriles and the spectral diffusion time constants and time compression factors (**Fig. 4**) reveal a roughly linear correlation (with differing slopes) with viscosity of the solvent, more noticeably so with the time compression factors. Viscosity of the solvent is also linearly dependent on the alkyl chain length (**SM**). Since both of these solvent properties are already correlated, a linear dependency between the spectral diffusion times and on the alkyl chain length of the solvent is also observed.

Comparison with Optical Kerr Effect Response of Pure Alkyl Nitriles

2D-IR spectroscopy accesses solvation dynamics of CMT in the alkyl nitriles, as well as in various other environments², from the perspective of a dissolved solute. For chemistry, this is the most relevant point of view because we are interested in how species such as catalysts, or catalyst-like molecules, interact with the surrounding solvent. It is, however, an impossible task to categorize every conceivable solvent-solute system individually, so the individual properties of the solute or solvent alone are useful to consider. The spectral diffusion time scales that we extract range from 1-5 ps, and, viewed as a window into the spectral density of the fluctuating environment, these raw time scales correspond to frequencies in the <100 cm⁻¹ range. Of course, our measurements can only access the dynamics of the probe frequency fluctuations, and any nonlinear mapping of the actual molecular dynamics to the vibrational frequency will lead to a difference in time scales of the FFCF. Low-frequency motions of liquids are characterized by collective intermolecular displacements and can be measured directly by virtue of their anisotropic polarizability using OKE spectroscopy. The Fourkas group has measured the OKE response of a diverse set of liquids, including all of the alkyl nitriles in this study.^{34,36} The collective orientational correlation

functions obtained from OKE spectroscopy are often modeled with two exponentials with time scales that differ by less than an order of magnitude. Here we will refer to the slower time component as the "collective orientational constant," and the faster component will be referred to as the "intermediate" decay.³⁴ There is some debate regarding the molecular origin of the intermediate decay, one proposal attributes the decay process to motionally narrowed low-frequency motions.³³ The Debye-Stokes Einstein relation suggests the collective orientational constant is directly proportional to the viscosity, which is demonstrated with the series of alkyl nitriles.^{33,34} Indeed, Fourkas *et al.* concluded that the dynamics observed in the OKE measurements support a rigid rod-like picture of the individual nitrile solvent molecules.³⁴

We anticipate that the viscosity dependent spectral diffusion of CMT arises from the same environmental fluctuations of the solvent that are captured by OKE spectroscopy. Plotting either the spectral diffusion time scales or the compression factors against the OKE collective orientational constants allows us to evaluate any possible relationships between spectral diffusion and orientational dynamics. A plot of the exponential spectral diffusion time constants versus collective orientational constants shows a positive correlation between the two variables (SM). The time compression factors (Fig. 5) reveal a nearly perfect linear correlation with the slow OKE time scale. Although all the variables also display a viscosity dependence, the remarkably linear correlation between the time compression factors and the collective orientational time constants highlights the connection between spectral diffusion and the

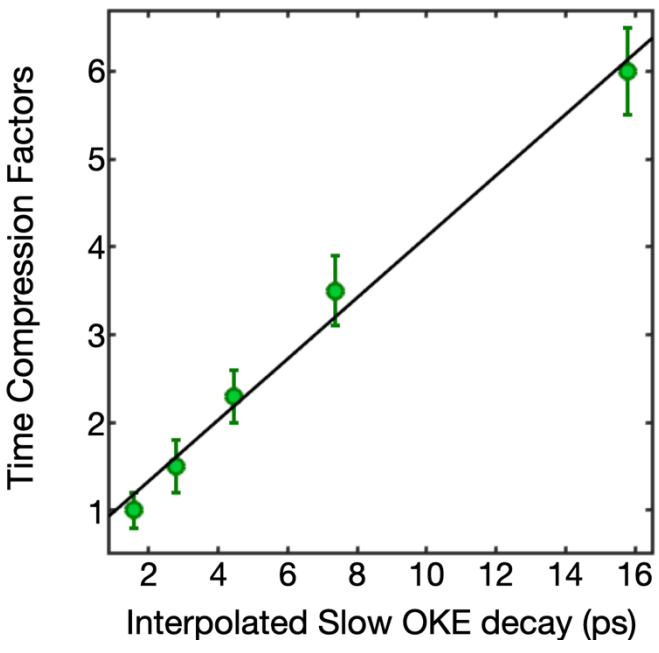


Figure 5. Correlation plot between time compression factors and interpolated collective orientational time constants at 298K. A line (black) is added to emphasize the linear correlation.

orientational dynamics of the solvent. It is also important to note that similar trends are observed with the intermediate decay times (**SM**). Although the slower component is the more dominant term in the collective orientational correlation function, both have been found to be strongly correlated, including the orientational times of the alkyl nitriles. These comparisons represent rather striking examples of how different perspectives on solvation dynamics can yield complementary information. 2D-IR is highly local to the solute, whereas OKE probes larger scale collective motions. We might expect such a concordance when the solute-solvent interactions are more specific and complex, such as the case when there is hydrogen bonding.

Intramolecular Vibrational Energy Redistribution Correlates with Collective Solvent Spectral Shifts

Intramolecular vibrational energy redistribution, or IVR, is a central topic in chemical physics research, occupying a cornerstone of statistical theories of chemical reaction rates. Much of the experimental access to IVR emerges from time-resolved electronic absorption spectroscopy, where line shape changes reflect the randomization of vibrational energy among excited states. In many of these measurements, the specific states involved in the IVR process are not well resolved or assigned. 2D-IR provides direct access to IVR in the condensed phase, and enables mode-specific IVR with high time and frequency resolution by monitoring the waiting-time dependent cross peak growth. 32,56,66-74

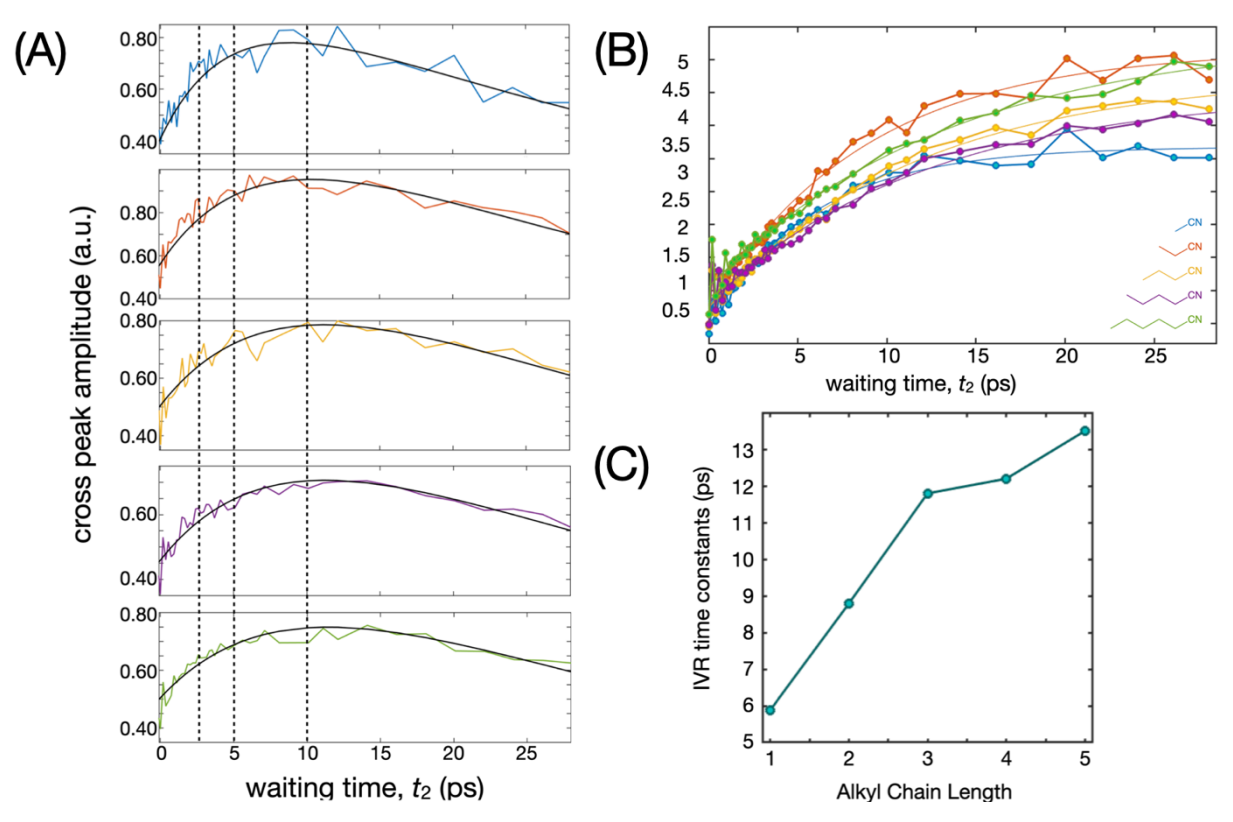


Figure 6. (A) Uphill cross peak amplitudes of CMT in each solvent. (B) Ratios of non-rephasing cross-peak to diagonal amplitudes are obtained and fitted to a single exponential to extract IVR times. Fitting the cross-peaks in (A) reveal similar IVR times obtained from fitting the ratios, assuming the vibrational relaxation time (T_1) and the initial value are not solvent-dependent. (C) Plotting alkyl chain length of the solvent versus the extracted IVR times reveals a positive correlation.

IVR time scales are extracted via the cross peak amplitudes (Fig. 6A). In this work, we use the cross peak in the upper left portion of the 2D spectrum (Fig. 2C), which arises due to excitation of the lower frequency band and detection of the higher frequency band. Non-rephasing cross peak amplitudes are divided by non-rephasing diagonal peak amplitudes to isolate the rising component of the cross peak, eliminating the overall vibrational relaxation (Fig. 6B). In principle, the cross peak rise due to the orientational relaxation is insignificant compared to the contribution of IVR.75 Polarization selective experiments are necessary to determine the time scales of the orientational relaxation times, however, our current experimental setup is optimized to measure the $R^{(3)}_{\scriptscriptstyle ZZZZ}$ and therefore the orientational relaxation time cannot be properly extracted at this time. Ratios of the cross peak and diagonal peak amplitudes are fitted to a single exponential with a constant offset (Fig. 6B), and the extracted IVR time constants are summarized in Table 1. Plotting the IVR times versus alkyl chain length exhibits a positive correlation (Fig. 6C). It is important to note that the cross peak examined (excited low mode, detected high mode) represents an "uphill" energy transfer, which is responsible for the modest 5-10 ps IVR time scale. In other words, the energy is transferring from the lower frequency mode to the higher frequency mode rather than the reverse direction, which is the more favored process. Ratios obtained from the other cross peak would most likely yield faster IVR times.

The solvent dependence of the IVR time scale is rather pronounced, increasing two-fold over the solvent series. The rates of IVR are directly proportional to the spectral density of the bath phonons at the energy mismatch between the coupled vibrations. The solvent contribution to the spectral density can be probed by OKE spectroscopy. Deconvolving the heterodyne detected OKE signal, and Fourier transforming

to the frequency domain, yields the low-frequency, anisotropic reduced spectral density (RSD). Quitevis *et al.* report RSDs of neat alkyl nitriles using OKE spectroscopy, using line shape analysis to separate interand intramolecular contributions.⁷⁶ The energy mismatch for the coupled vibrations of CMT is approximately 90 cm⁻¹ in all of the nitriles, thus the IVR time scales are related to the RSD of the liquid phonon modes at this energy mismatch.

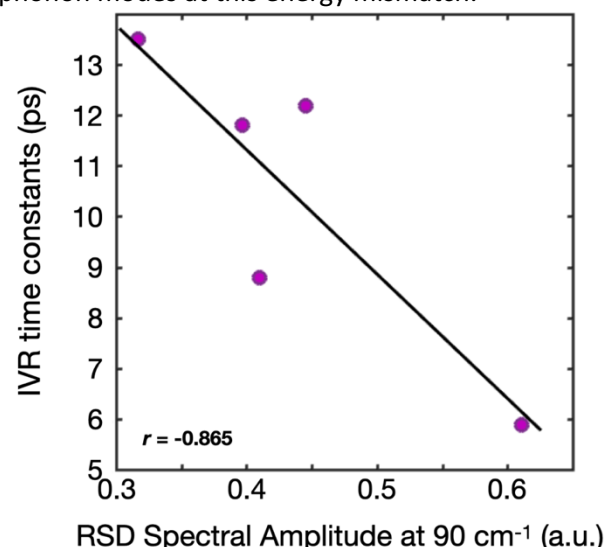


Figure 7. Correlation plot of RSD spectral amplitudes (from Ref. 42) against IVR times reveals a relatively strong anticorrelation between the two variables, yielding a correlation coefficient (r) of -0.865. A black line is added to emphasize the linear correlation.

Based on fitting results of the RSDs, we can compare various aspects of the intermolecular density of states to our IVR time constants. Quitevis et al. use a set of line shapes to represent various spectral ranges; a Bucaro-Litovitz (BL) line shape for the lowest frequency region accounts for collisioninduced light scattering, and an anti-symmetrized-Gaussian (AG) is attributed to librational motions. 40,77 RSD spectra of polar solvents are primarily dominated by librational motions.⁷⁷ The full RSD is fit with one BL and five AG line shape contributions, of which three lowest bands constitute the intermolecular spectral density. The amplitude of the intermolecular constructed from those three lowest frequency bands show a strong anti-correlation with our observed IVR rate constants, yielding a correlation coefficient (r) of -0.865 (Fig. 7). This comparison shows that as the RSD amplitude decreases as the solvent bath spectrum shifts out of resonance with our 90-cm⁻¹ vibrational energy gap, the IVR slows

down, which is the expectation from Fermi's golden rule.

Finally, we use these findings to reconsider previous results we obtained using the Re(bpy)(CO)₃Cl CO₂ reduction catalyst in a series of solvents. In that work, we studied several derivatives of the rhenium complex with different substitutions on the bipyridyl ligand (as well as phenanthroline) and found essentially no structural influence on the spectral diffusion time scales. For the basic molecule Re(bpy)(CO)₃Cl, we found that solvent dictates the dynamics time scale, with DMSO (4.2 ps) > ACN(1.6 ps) > THF (1.3 ps), correlating with the solvent donor number as well as with the bulk solvent viscosity. From OKE spectroscopy, the collective orientational constants for these solvents are DMSO (6.85 ps) > ACN (1.6 ps) > THF (1.1 ps), which is consistent with our spectral diffusion trend. Si, 36,78 Given that the OKE data are fitted using multiple exponentials, there is no doubt some non-uniqueness to those time constants. There is also some spread in the spectral diffusion values obtained using 2D-IR among the different derivatives, so it seems reasonable to conclude that our spectral diffusion results are consistent with the orientational dynamics time scale obtained with OKE. A plot showing the comparison of spectral diffusion time scales Re(bpy)(CO)₃Cl in various solvents (**SM**).

CONCLUSION

Using a catalyst-like transition metal carbonyl complex as a spectroscopic probe, we find both spectral diffusion and IVR depend on solvent chain length in a series of alkyl nitriles. Similar to our previous work in a series of linear alcohols, we find a monotonic increase in spectral diffusion time scales with increased alkyl chain length. Although this correlation tracks with bulk solvent viscosity, we argue the better comparison is with the orientational dynamics of the solvent obtained directly by optical Kerr effect spectroscopy. IVR, which is governed by intramolecular coupling and the density of states of low-

frequency modes, correlates with the residual spectral density amplitude at the frequency difference, also determined using OKE spectroscopy. As previously investigated in the context of dynamic Stokes shifts, we find a potentially useful complementarity of 2D-IR dynamics and spectral information available from OKE (or THz). Future work to push the limits of this complementarity will be useful, especially in more complex solvation environments and in solvent mixtures that are very common in chemical synthesis.

SUPPLEMENTARY MATERIALS

See the supplementary materials for rephasing and non-rephasing amplitudes for CMT in each solvent; a correlation plot of viscosity and chain length for the alkyl nitriles; explanations of how error bars for the spectral diffusion times and time compression factors are determined; plots of spectral diffusion times and time compression factors against the collective orientational times and the intermediate times; and an analysis of comparing the spectral dynamics of rhenium tricarbonyl complexes to orientational dynamics of the solvents (ACN, THF, and DMSO).

ACKNOWLEDGEMENTS

This work was supported by the National Science Foundation (CHE-1836529 and CHE-1955026). This material is based upon work supported by the National Science Foundation Graduate Research Fellowship (V.F.C, DGE 1841052). We are grateful to E. Quitevis and D. Meng for sharing their unpublished OKE results that we have used to compare to our data.

DATA AVAILABILITY

The data that support the findings of this study are available from the corresponding author upon reasonable request.

REFERENCES

- ¹ J.T. King, C.R. Baiz, and K.J. Kubarych, *Solvent-Dependent Spectral Diffusion In A Hydrogen Bonded "Vibrational Aggregate."* J. Phys. Chem. A **114**, 10590 (2010).
- ² D.G. Osborne, J.T. King, J.A. Dunbar, A.M. White, and K.J. Kubarych, *Ultrafast 2DIR Probe Of A Host-Guest Inclusion Complex: Structural And Dynamical Constraints Of Nanoconfinement*. J. Chem. Phys. **138**, 144501 (2013).
- ³ C.J. Huber, T.C. Anglin, B.H. Jones, N. Muthu, C.J. Cramer, and A.M. Massari, *Vibrational Solvatochromism In Vaska's Complex Adducts*. J. Phys. Chem. A **116**, 9279 (2012).
- ⁴ B.H. Jones, C.J. Huber, and A.M. Massari, *Solvation Dynamics Of Vaska's Complex By 2D-IR Spectroscopy*. J. Phys. Chem. C **115**, 24813 (2011).
- ⁵ J.T. King, M.R. Ross, and K.J. Kubarych, *Ultrafast α-Like Relaxation Of A Fragile Glass-Forming Liquid Measured Using Two-Dimensional Infrared Spectroscopy*. Phys. Rev. Lett. **108**, 157401 (2012).
- ⁶ J.T. King and K.J. Kubarych, *Site-Specific Coupling Of Hydration Water And Protein Flexibility Studied In Solution With Ultrafast 2D-IR Spectroscopy*. J. Am. Chem. Soc. **134**, 18705 (2012).
- ⁷ K. Kwak, S. Park, and M.D. Fayer, *Dynamics Around Solutes And Solute–Solvent Complexes In Mixed Solvents*. Proc. Natl. Acad. Sci. **104**, 14221 LP (2007).
- ⁸ D.B. Wong, K.P. Sokolowsky, M.I. El-Barghouthi, E.E. Fenn, C.H. Giammanco, A.L. Sturlaugson, and M.D. Fayer, *Water Dynamics In Water/DMSO Binary Mixtures*. J. Phys. Chem. B **116**, 5479 (2012).
- ⁹ J.A. Dunbar, E.J. Arthur, A.M. White, and K.J. Kubarych, *Ultrafast 2D-IR And Simulation Investigations Of Preferential Solvation And Cosolvent Exchange Dynamics*. J. Phys. Chem. B **119**, 6271 (2015).
- ¹⁰ B.M. Luther, J.R. Kimmel, and N.E. Levinger, *Dynamics Of Polar Solvation In Acetonitrile–Benzene Binary Mixtures: Role Of Dipolar And Quadrupolar Contributions To Solvation*. J. Chem. Phys. **116**, 3370 (2002).

- ¹¹ D. Chakrabarty, A. Chakraborty, D. Seth, and N. Sarkar, *Effect Of Water, Methanol, And Acetonitrile On Solvent Relaxation And Rotational Relaxation Of Coumarin 153 In Neat 1-Hexyl-3-Methylimidazolium Hexafluorophosphate*. J. Phys. Chem. A **109**, 1764 (2005).
- ¹² C.N. Nguyen and R.M. Stratt, *Preferential Solvation Dynamics In Liquids: How Geodesic Pathways Through The Potential Energy Landscape Reveal Mechanistic Details About Solute Relaxation In Liquids*. J. Chem. Phys. **133**, 124503 (2010).
- ¹³ N. Agmon, *The Dynamics Of Preferential Solvation*. J. Phys. Chem. A **106**, 7256 (2002).
- ¹⁴ L.M. Kiefer and K.J. Kubarych, *Solvent Exchange In Preformed Photocatalyst-Donor Precursor Complexes Determines Efficiency*. Chem. Sci. **9**, 1527 (2018).
- ¹⁵ L.M. Kiefer and K.J. Kubarych, *Solvent-Dependent Dynamics Of A Series Of Rhenium Photoactivated Catalysts Measured With Ultrafast 2DIR.* J. Phys. Chem. A **119**, 959 (2015).
- ¹⁶ A. Ghosh, A. Remorino, M.J. Tucker, and R.M. Hochstrasser, *2D IR Photon Echo Spectroscopy Reveals Hydrogen Bond Dynamics Of Aromatic Nitriles*. Chem. Phys. Lett. **469**, 325 (2009).
- ¹⁷ N. Sagawa and T. Shikata, *Dangling OH Vibrations Of Water Molecules In Aqueous Solutions Of Aprotic Polar Compounds Observed In The Near-Infrared Regime*. J. Phys. Chem. B **119**, 8087 (2015).
- ¹⁸ Y.S. Kim and R.M. Hochstrasser, *Chemical Exchange 2D IR Of Hydrogen-Bond Making And Breaking*. Proc. Natl. Acad. Sci. **102**, 11185 (2005).
- ¹⁹ R.C. Larson and R.T. Iwamoto, *Solvent Effects On The Polarographic Reduction Of Metal Ions. II. Nitrile Solvents*. J. Am. Chem. Soc. **82**, 3526 (1960).
- ²⁰ J. Neuhaus, E. von Harbou, and H. Hasse, *Physico-Chemical Properties Of LiFSI Solutions I. LiFSI With Valeronitrile, Dichloromethane, 1,2-Dichloroethane, And 1,2-Dichlorobenzene*. J. Chem. Eng. Data **64**, 868 (2019).
- ²¹ J.P. Dinnocenzo, J. Tingson, R.H. Young, and S. Farid, *Solvent Dependence Of Cationic-Exciplex Emission: Limitation Of Solvent Polarity Functions And The Role Of Hydrogen Bonding*. J. Phys. Chem. A **124**, 3730 (2020).
- ²² T.O. Harju, J.E.I. Korppi-Tommola, A.H. Huizer, and C.A.G.O. Varma, *Barrier Crossing Reaction Of Electronically Excited DBMBF*₂ *In* N-Nitriles: The Role Of Solvent Polarity On Activation Energy. J. Phys. Chem. **100**, 3592 (1996).
- ²³ B. Li and K.S. Peters, *Application Of Kramers Theory To The Diffusional Separation Of The Trans-Stilbene/Fumaronitrile Contact Radical Ion Pair In Alkyl Nitrile Solvents*. J. Phys. Chem. **97**, 7648 (1993).
- ²⁴ K.S. Peters and G. Kim, Solvent Effects For Nonadiabatic Proton Transfer In The Benzophenone/N,N-Dimethylaniline Contact Radical Ion Pair. J. Phys. Chem. A **105**, 4177 (2001).
- ²⁵ E. Vauthey, Isomerisation Dynamics Of A Thiacarbocyanine Dye In Different Electronic States And In Different Classes Of Solvents. Chem. Phys. **196**, 569 (1995).
- ²⁶ D.R. Bessire and E.L. Quitevis, *Effect Of Temperature And Viscosity On Rotational Diffusion Of Merocyanine 540 In Polar Solvents*. J. Phys. Chem. **98**, 13083 (1994).
- ²⁷ E.K.L. Yeow and S.E. Braslavsky, *Quenching Of Zinc Tetraphenylporphine By Oxygen And By 1,4-Benzoquinone In Nitrile Solvents: An Optoacoustic Spectroscopy Study*. Phys. Chem. Chem. Phys. **4**, 239 (2002).
- ²⁸ T. Uzer and W.H. Miller, *Theories Of Intramolecular Vibrational Energy Transfer*. Phys. Rep. **199**, 73 (1991).
- ²⁹ J.C. Owrutsky, D. Raftery, and R.M. Hochstrasser, *Vibrational Relaxation Dynamics In Solutions*. Annu. Rev. Phys. Chem. **45**, 519 (1994).
- ³⁰ A. Tokmakoff, B. Sauter, and M.D. Fayer, *Temperature-dependent Vibrational Relaxation In Polyatomic Liquids: Picosecond Infrared Pump–Probe Experiments.* J. Chem. Phys. **100**, 9035 (1994).
- ³¹ J.F. Cahoon, K.R. Sawyer, J.P. Schlegel, and C.B. Harris, *Determining Transition-State Geometries In Liquids Using 2D-IR*. Science **319**, 1820 (2008).
- ³² J.T. King, J.M. Anna, and K.J. Kubarych, *Solvent-Hindered Intramolecular Vibrational Redistribution*.

- Phys. Chem. Chem. Phys. 13, 5579 (2011).
- ³³ Q. Zhong and J.T. Fourkas, *Optical Kerr Effect Spectroscopy Of Simple Liquids*. J. Phys. Chem. B **112**, 15529 (2008).
- ³⁴ X. Zhu, R.A. Farrer, Q. Zhong, and J.T. Fourkas, *Orientational Diffusion Of N-Alkyl Cyanides*. J. Phys. Condens. Matter **17**, S4105 (2005).
- ³⁵ Q. Zhong and J.T. Fourkas, *Searching For Voids In Liquids With Optical Kerr Effect Spectroscopy*. J. Phys. Chem. B **112**, 8656 (2008).
- ³⁶ B.J. Loughnane, A. Scodinu, R.A. Farrer, J.T. Fourkas, and U. Mohanty, *Exponential Intermolecular Dynamics In Optical Kerr Effect Spectroscopy Of Small-Molecule Liquids*. J. Chem. Phys. **111**, 2686 (1999).
- ³⁷ B.J. Berne, J.T. Fourkas, R.A. Walker, and J.D. Weeks, *Nitriles At Silica Interfaces Resemble Supported Lipid Bilayers*. Acc. Chem. Res. **49**, 1605 (2016).
- ³⁸ M. Cho, S.J. Rosenthal, N.F. Scherer, L.D. Ziegler, and G.R. Fleming, *Ultrafast Solvent Dynamics: Connection Between Time Resolved Fluorescence And Optical Kerr Measurements*. J. Chem. Phys. **96**, 5033 (1992).
- ³⁹ J.S. Bender, B. Coasne, and J.T. Fourkas, *Assessing Polarizability Models For The Simulation Of Low-Frequency Raman Spectra Of Benzene*. J. Phys. Chem. B **119**, 9345 (2015).
- ⁴⁰ D. Meng, S. Sagala, A.J.A. Aquino, and E.L. Quitevis, *Orientational And Low-Frequency (0–450 Cm⁻¹) Dynamics Of Methyl Methacrylate: OHD-RIKES Measurements And DFT Calculations*. J. Mol. Liq. **323**, 115004 (2021).
- ⁴¹ L.M. Kiefer and K.J. Kubarych, *Two-Dimensional Infrared Spectroscopy Of Coordination Complexes: From Solvent Dynamics To Photocatalysis*. Coord. Chem. Rev. **372**, 153 (2018).
- ⁴² C.R. Baiz, P.L. McRobbie, J.M. Anna, E. Geva, and K.J. Kubarych, *Two-Dimensional Infrared Spectroscopy Of Metal Carbonyls*. Acc. Chem. Res. **42**, 1395 (2009).
- ⁴³ I. Rémy, P. Brossier, I. Lavastre, J. Besançon, and C. Moïse, *Potentiality Of An Organometallic Labelled Streptavidin—Biotin System In Metalloimmunoassay*. J. Pharm. Biomed. Anal. **9**, 965 (1991).
- ⁴⁴ I. Rémy and P. Brossier, *Atomic Absorption Spectrometric Detection Of Biotin-Cymantrene As A Metallo-Tracer For The Avidin–Biotin System*. Analyst **118**, 1021 (1993).
- ⁴⁵ S. Clède, F. Lambert, C. Sandt, Z. Gueroui, M. Réfrégiers, M.-A. Plamont, P. Dumas, A. Vessières, and C. Policar, *A Rhenium Tris-Carbonyl Derivative As A Single Core Multimodal Probe For Imaging (SCoMPI) Combining Infrared And Luminescent Properties*. Chem. Commun. **48**, 7729 (2012).
- ⁴⁶ A.M. Woys, S.S. Mukherjee, D.R. Skoff, S.D. Moran, and M.T. Zanni, *A Strongly Absorbing Class Of Non-Natural Labels For Probing Protein Electrostatics And Solvation With FTIR And 2D IR Spectroscopies*. J. Phys. Chem. B **117**, 5009 (2013).
- ⁴⁷ J.M. Anna, M.J. Nee, C.R. Baiz, R. McCanne, and K.J. Kubarych, *Measuring Absorptive Two-Dimensional Infrared Spectra Using Chirped-Pulse Upconversion Detection*. J. Opt. Soc. Am. B **27**, 382 (2010).
- ⁴⁸ C.R. Baiz and K.J. Kubarych, *Ultrabroadband Detection Of A Mid-IR Continuum By Chirped-Pulse Upconversion*. Opt. Lett. **36**, 187 (2011).
- ⁴⁹ R. Duan, J.N. Mastron, Y. Song, and K.J. Kubarych, *Direct Comparison Of Amplitude And Geometric Measures Of Spectral Inhomogeneity Using Phase-Cycled 2D-IR Spectroscopy*. J. Chem. Phys. **154**, 174202 (2021).
- ⁵⁰ C.R. Baiz, K.J. Kubarych, E. Geva, and E.L. Sibert, *Local-Mode Approach To Modeling Multidimensional Infrared Spectra Of Metal Carbonyls*. J. Phys. Chem. A **115**, 5354 (2011).
- ⁵¹ S. Park, K. Kwak, and M.D. Fayer, *Ultrafast 2D-IR Vibrational Echo Spectroscopy: A Probe Of Molecular Dynamics*. Laser Phys. Lett. **4**, 704 (2007).
- ⁵² J.B. Asbury, T. Steinel, and M.D. Fayer, *Vibrational Echo Correlation Spectroscopy Probes Of Hydrogen Bond Dynamics In Water And Methanol.* J. Lumin. **107**, 271 (2004).
- ⁵³ P.F. Tekavec, J.A. Myers, K.L.M. Lewis, and J.P. Ogilvie, *Two-Dimensional Electronic Spectroscopy With A Continuum Probe*. Opt. Lett. **34**, 1390 (2009).

- ⁵⁴ R. Torre, P. Bartolini, M. Ricci, and R.M. Pick, *Time-Resolved Optical Kerr Effect On A Fragile Glass-Forming Liquid: Test Of Different Mode Coupling Theory Aspects*. Europhys. Lett. **52**, 324 (2000).
- ⁵⁵ R. Torre, P. Bartolini, and R. Righini, *Structural Relaxation In Supercooled Water By Time-Resolved Spectroscopy*. Nature **428**, 296 (2004).
- ⁵⁶ J.M. Anna and K.J. Kubarych, *Watching Solvent Friction Impede Ultrafast Barrier Crossings: A Direct Test Of Kramers Theory*. J. Chem. Phys. **133**, 174506 (2010).
- ⁵⁷ N. Sivakumar, E.A. Hoburg, and D.H. Waldeck, *Solvent Dielectric Effects On Isomerization Dynamics: Investigation Of The Photoisomerization Of 4,4'-dimethoxystilbene And T-stilbene In N-alkyl Nitriles*. J. Chem. Phys. **90**, 2305 (1989).
- ⁵⁸ B.J. Loughnane, A. Scodinu, and J.T. Fourkas, *Temperature-Dependent Optical Kerr Effect Spectroscopy Of Aromatic Liquids*. J. Phys. Chem. B **110**, 5708 (2006).
- ⁵⁹ Q. Zhong and J.T. Fourkas, *Shape And Electrostatic Effects In Optical Kerr Effect Spectroscopy Of Aromatic Liquids*. J. Phys. Chem. B **112**, 15342 (2008).
- ⁶⁰ Q. Zhong, X. Zhu, and J.T. Fourkas, *Temperature-Dependent Orientational Dynamics Of 1,N-Dicyano N-Alkanes*. J. Phys. Chem. B **112**, 3115 (2008).
- ⁶¹ C. Zhang, E.L. Sibert, and M. Gruebele, *A Phase Diagram For Energy Flow-Limited Reactivity*. J. Chem. Phys. **154**, 104301 (2021).
- ⁶² S. Karmakar and S. Keshavamurthy, *Intramolecular Vibrational Energy Redistribution And The Quantum Ergodicity Transition: A Phase Space Perspective*. Phys. Chem. Chem. Phys. **22**, 11139 (2020).
- ⁶³ K.F. Freed and A. Nitzan, *Intramolecular Vibrational Energy Redistribution And The Time Evolution Of Molecular Fluorescence*. J. Chem. Phys. **73**, 4765 (1980).
- ⁶⁴ K.F. Freed, Irreversible Electronic Relaxation In Polyatomic Molecules. J. Chem. Phys. **52**, 1345 (1970).
- ⁶⁵ D.W. Lupo and M. Quack, *IR-Laser Photochemistry*. Chem. Rev. **87**, 181 (1987).
- ⁶⁶ X. Dong, F. Yang, J. Zhao, and J. Wang, Efficient Intramolecular Vibrational Excitonic Energy Transfer In Ru₃(CO)₁₂ Cluster Revealed By Two-Dimensional Infrared Spectroscopy. J. Phys. Chem. B **122**, 1296 (2018).
- ⁶⁷ P.A. Eckert and K.J. Kubarych, *Dynamic Flexibility Of Hydrogenase Active Site Models Studied With 2D-IR Spectroscopy*. J. Phys. Chem. A **121**, 608 (2017).
- ⁶⁸ P.A. Eckert and K.J. Kubarych, *Oxidation-State-Dependent Vibrational Dynamics Probed With 2D-IR*. J. Phys. Chem. A **121**, 2896 (2017).
- ⁶⁹ P.A. Eckert and K.J. Kubarych, *Solvent Quality Controls Macromolecular Structural Dynamics Of A Dendrimeric Hydrogenase Model*. J. Phys. Chem. B **122**, 12154 (2018).
- ⁷⁰ P.A. Eckert and K.J. Kubarych, *Vibrational Coherence Transfer Illuminates Dark Modes In Models Of The FeFe Hydrogenase Active Site*. J. Chem. Phys. **151**, 54307 (2019).
- ⁷¹ J.M. Anna, M.R. Ross, and K.J. Kubarych, *Dissecting Enthalpic And Entropic Barriers To Ultrafast Equilibrium Isomerization Of A Flexible Molecule Using 2DIR Chemical Exchange Spectroscopy*. J. Phys. Chem. A **113**, 6544 (2009).
- ⁷² J.M. Anna, J.T. King, and K.J. Kubarych, *Multiple Structures And Dynamics Of* [$CpRu(CO)_2$]₂ And [$CpFe(CO)_2$]₂ In Solution Revealed With Two-Dimensional Infrared Spectroscopy. Inorg. Chem. **50**, 9273 (2011).
- 73 F. Yang, X. Dong, M. Feng, J. Zhao, and J. Wang, Central-Metal Effect On Intramolecular Vibrational Energy Transfer Of M(CO)5Br (M = Mn, Re) Probed By Two-Dimensional Infrared Spectroscopy. Phys. Chem. Chem. Phys. **20**, 3637 (2018).
- 74 F. Yang, J. Zhao, and J. Wang, *Two-Dimensional Infrared Study Of* 13 C-Natural Abundant Vibrational Transition Reveals Intramolecular Vibrational Redistribution Rather Than Fluxional Exchange In $Mn(CO)_5$ Br. J. Phys. Chem. B **120**, 1304 (2016).
- ⁷⁵ O. Golonzka and A. Tokmakoff, *Polarization-Selective Third-Order Spectroscopy Of Coupled Vibronic States*. J. Chem. Phys. **115**, 297 (2001).

⁷⁶ D. Meng, S. Sagala, and E.L. Quitevis, *Effect Of Alkyl Chain Length On The Low-Frequency Intramolecular Dynamics Of N-Alkyl Nitriles: OHD RIKES Measurements And DFT Calculations. Effect of Alkyl Chain Length on the Low-Frequency Intramolecular Dynamics of n-Alkyl Nitriles: OHD RIKES Measurements and DFT Calculations* (n.d.).

⁷⁷ J. Rajesh Rajian, S. Li, R.A. Bartsch, and E.L. Quitevis, *Temperature-Dependence Of The Low-Frequency Spectrum Of 1-Pentyl-3-Methylimidazolium Bis(Trifluoromethanesulfonyl)Imide Studied By Optical Kerr Effect Spectroscopy*. Chem. Phys. Lett. **393**, 372 (2004).

⁷⁸ P.P. Wiewiór, H. Shirota, and E.W. Castner, *Aqueous Dimethyl Sulfoxide Solutions: Inter- And Intra-Molecular Dynamics*. J. Chem. Phys. **116**, 4643 (2002).